A comparison of the structure of lamellar stacks in a semicrystalline polymer during melting and crystallization by means of the Intensity Superposition Method*)

Stanisław Rabiej[1), **)], **Małgorzata Rabiej**[1)]

Abstract: This work presents the results of Small Angle X-ray Scattering (SAXS) investigations of the structure of lamellar stacks in ethylene-1-octene copolymer during heating and cooling. The SAXS curves were analysed using the Intensity Superposition Method (ISM). By means of this method, not only the average values of the parameters of lamellar stacks but also the stacks crystallinity distribution function were determined. Based on this function, the structure of lamellar stacks during crystallization and melting of the copolymer was compared and observed differences were indicated.

Keywords: SAXS, lamella, crystallinity, distribution.

Porównanie struktury stosów lamelarnych w semikrystalicznym polimerze w trakcie topnienia i krystalizacji za pomocą Metody Superpozycji Intensywności

Streszczenie: Przedstawiono wyniki badań struktury stosów lamelarnych w kopolimerach etylen--1-okten, wykonane metodą małokątowego rozpraszania promieni rentgenowskich (SAXS) w trakcie ogrzewania i chłodzenia. Krzywe SAXS analizowano przy użyciu Metody Superpozycji Intensywności (ISM). Metoda ta pozwoliła wyznaczyć nie tylko średnie wartości parametrów stosów, ale także funkcję rozkładu stopnia krystaliczności stosów. Na podstawie analizy tej funkcji wykazano istotne różnice w strukturze stosów lamelarnych w procesach krystalizacji i topnienia.

Słowa kluczowe: SAXS, lamela, stopień krystaliczności, rozkład.

From the point of view of the Small Angle X-ray Scattering (SAXS) method the supermolecular structure of semicrystalline polymers can be analysed as an isotropic system of lamellar stacks formed of alternating crystalline lamellae and amorphous layers. The fundamental parameters of stacks *i.e.*: average long period, thicknesses of crystalline lamellae and amorphous layers and volume crystallinity can be determined in two ways. The first one consists in application of the theory derived by Strobl & Schneider [1] and Vonk & Kortleve [2] and calculation of so called one dimensional correlation function.

Alternatively, the structure of lamellar stacks can be determined by construction of a theoretical intensity function, related to an assumed model of lamellar stacks, and

best fitted to a given experimental SAXS curve. The simplest model of the lamellar stacks structure (Single Stack Model) in a polymer, assumes that all stacks are statistically identical. It means that all of them are characterized by the same average values of amorphous layer thickness A_0, average crystalline lamella thickness C_0 and average long period L_0, where $L_0 = A_0 + C_0$. The thicknesses of crystals and amorphous layers fluctuate independently on one another and they are described by independent distribution functions $G_A(A)$ and $G_C(C)$ but in all stacks the distributions are the same. In such a case, the one dimensional intensity distribution function $I_1(s)$ describing the intensity scattered perpendicularly to the layers of stacks is given by the formula given by Hermans [3] and Hosemann [4]:

$$I_1(s) = K\frac{\varphi}{sC_0} \cdot \frac{1 - \left|F_L\right|^2 - \left|F_C\right|\left(1 - \left|F_A\right|^2\right)\cos\left(2\pi sC_0\right) - \left|F_A\right|\left(1 - \left|F_C\right|^2\right)\cos\left\{2\pi s\left[C_0\frac{1-\varphi}{\varphi}\right]\right\}}{1 - 2\left|F_L\right|\cos\left[2\pi s\frac{C_0}{\varphi}\right] + \left|F_L\right|^2} \cdot T(s) \qquad (1)$$

where: $s = 2\sin\theta/\lambda$ is the scattering vector, F_C and F_A are Fourier transforms of the thickness distributions of crystalline lamellae $G_C(C)$ and amorphous layers $G_A(A)$, $F_L = F_C \cdot F_A$, $\varphi = C_0/L_0$ is the average volume crystallinity of the stack and K is the scaling constant.

Usually it is assumed that the thickness distributions of stacks $G_A(C)$ and $G_C(A)$ are Gauss functions with the standard deviations σ_C and σ_A, respectively. Their Fourier transforms are equal to:

$$F_A = \exp(-2\pi^2 s^2 \sigma_A^2)\exp(2\pi s i A_0)$$

$$\tag{2}$$

$$F_C = \exp(-2\pi^2 s^2 \sigma_C^2)\exp(2\pi s i C_0)$$

$T(s)$ is a factor related to the transition zone at the phase boundaries. According to Ruland [5], for a sigmoidal electron density profile across the interface the $T(s)$ is given by:

$$T(s) = \exp(-4\pi^2 \delta^2 s^2) \tag{3}$$

where δ is a parameter related to the thickness of the transition zone between the crystalline and amorphous layers.

As it has been shown in our former paper [6] the Single Stack Model can be successfully employed for the isothermally crystallized polymers. However it is too simplified when the crystallization temperature is variable. In our next studies [7, 8] it was shown that the structure of stacks formed at different temperatures is not the same and the degree of crystallinity of stacks clearly depends on the crystallization temperature. As a result it is impossible to fit the theoretical SAXS curves based on the Single Stack Model to the experimental ones. For this reason more complex models of polymer structure must be used in the analysis of the SAXS curves of non-isothermally crystallized polymers. The Intensity Superposition Method proposed by Blundell [9] is one of possible solutions. In this method, the total scattered intensity per unit volume of a polymer is presented as a superposition of intensities scattered by stacks of various crystallinity

$$I_1(s) = \int_0^1 I_1(s,\varphi) \cdot P(\varphi)\,\mathrm{d}\varphi \tag{4}$$

where: $I_1(s,\varphi)$ is the intensity scattered by a stack of the volume crystallinity φ, given by equation (1) and $P(\varphi)$ is a normalized distribution function describing the contribution of such stacks to the total intensity $I_1(s)$.

Off course, determination of the $P(\varphi)$ distribution function which assures a god fit of the theoretical function $I_1(s)$ [Eq. (4)] to the experimental curves is one of the most important points of the method.

It is worth to emphasize that employing the Intensity Superposition Method we can find not only the average values of the parameters of stacks but we gain quantitative data on the homogeneity of investigated polymer. Observing and analyzing the shape of the $P(\varphi)$ function we obtain additional and unique information on the

changes in the structure of stacks during various processes.

In our previous work [8] we have used this method in the investigations of the crystallization process of homogeneous ethylene-1-octene copolymer during cooling at a constant rate from the melt down to room temperature.

In this work we employed the Intensity Superposition Method for tracing the changes in the structure of the same copolymer during heating from room temperature up to complete melting. We aimed at a comparison of the transformations in the structure of stacks during melting and crystallization analyzing the changes in the shape and parameters of the $P(\varphi)$ distribution function. The investigations have shown that the structure of lamellar stacks during crystallization and melting is clearly different.

EXPERIMENTAL PART

Materials

The investigations were performed for homogeneous ethylene-1-octene copolymer with 5.2 mol% of 1-octene, produced by DSM (The Netherlands).

Methodology

At first, the copolymer was melted at 150°C and after 5 min it was cooled at a constant rate of 10°C/min. SAXS curves were recorded every 2°C. The temperature of the sample was controlled by the Mettler FP-82HT hot stage. First analyzed curve was recorded at 89.5°C and the last at 25.5°C. Obtained results are described in our former paper [8].

In the second stage the copolymer was heated at the rate of 10°C/min from 25.5°C up to 150°C. SAXS curves were recorded every 2°C in the range 25.5–101.5°C. The time resolved synchrotron measurements were performed at EMBL laboratory of DESY in Hamburg.

First step of the experimental SAXS curves elaboration included all necessary corrections, normalization, melt pattern subtraction and smoothing. Next a constant background scattering, caused by the electron density fluctuations within the phases was determined and subtracted from the curves using the method of Koberstein *et al.* [10]. Finally, the experimental curves $I(s)$ were transformed into one-dimensional scattering curves $I_1(s)$ by Lorentz correction [11]:

$$I_1(s) = 4\pi s^2 I(s) \tag{5}$$

Theoretical intensity functions described by Eq. (4) were best fitted to the experimental one-dimensional scattering curves using the least squares method. The curves were fitted using the non-linear optimization procedure [12]. In this way $P(\varphi)$ function and the parameters of stacks were determined.

Additionally, to check if the obtained results are correct, the parameters of stacks were obtained from one-

dimensional correlation function which was calculated and analyzed for each curve using the method developed by Strobl & Schneider [1].

All calculations were performed using our computer program SAXDAT [13].

Modelling

The results of our former works [6–8] indicated that investigated copolymer is inhomogeneous in terms of the structure of lamellar stacks, *i.e.* the stacks differs in their volume crystallinity. Consequently, we assumed that the total intensity scattered by the copolymer can be presented by Eq. (4), as a superposition of intensities scattered by stacks of various crystallinity φ. In this equation, the one-dimensional intensity $I_1(s,\varphi)$ scattered by a stack of the volume crystallinity φ is described by Eq. (1) with the related Eq. (2) and Eq. (3), and $P(\varphi)$ is a normalized distribution function describing the contribution of such stacks to the total intensity $I_1(s)$.

Similarly as in our former investigations of the cooling stage [8] we assumed that:

– so called zero order scattering of stacks is below experimentally accessed range of angles and can be neglected [4, 9].

– the reduced standard deviations of the crystalline and amorphous layer thickness distributions are equal to each other [9]:

$$\frac{\sigma_C}{C_0} = \frac{\sigma_A}{A_0} = g \qquad (6)$$

and the maximum value of the reduced standard deviation is $g \leq 1/3$

– the average thickness C_0 of crystalline lamellae is the same in all stacks. So, different crystallinity of various stacks means different average thickness of amorphous layers and consequently different long period,

– the $P(\varphi)$ distribution function is a positively skewed split Gauss function.

$$\varphi \leqslant \varphi_m \ \ P(\varphi) = \frac{2}{\sigma\sqrt{2\pi}(n+1)}\exp\left[\frac{-(\varphi-\varphi_m)^2}{2\sigma^2}\right]$$

$$\varphi > \varphi_m \ \ P(\varphi) = \frac{2}{\sigma\sqrt{2\pi}(n+1)}\exp\left[\frac{-(\varphi-\varphi_m)^2}{2n^2\sigma^2}\right] \qquad (7)$$

were φ_m is the value of φ for which $P(\varphi)$ reaches its maximum.

Split Gauss function is constructed as a normalized combination of two "half Gauss" functions [Eq. (7)]. Standard deviation on its left and right sides amounts to σ and $n\sigma$, respectively. The asymmetry factor n determines the asymmetry of distribution. As the probability function $P(\varphi)$ must be normalized to unity and crystallinity must meet a condition: $0 \leq \varphi \leq 1$, the following

two constraints are imposed on the parameters: σ, n and φ_m : $\varphi_m \geq 3\sigma$ and $1 - \varphi_m \geq 3n\sigma$.

The theoretical functions $I_1(s)$ constructed according to the rules presented above were best fitted to the experimental curves using the least squares method. In the fitting procedure six independent parameters of this function were optimized. Three parameters are related to the distribution function $P(\varphi)$ [Eq. (7)]: the value φ_m for which $P(\varphi)$ reaches its maximum, standard deviation σ and the asymmetry factor n. The remaining three parameters are related to the intensity scattered by one stack $I_1(s,\varphi)$ [Eq. (1)]: average thickness of crystalline lamellae C_0, reduced standard deviation g and the transition layer parameter δ.

RESULTS AND DISCUSSION

Performed calculations have shown that the $P(\varphi)$ distribution function of the form given by Eq. (7) assures a good fit of the theoretical function $I_1(s)$ [Eq. (4)] to the experimental curves recorded during heating of the copolymer in the range 25.5–93.5°C. Some examples are shown in Figs. 1–3.

They present the experimental one–dimensional scattering curves recorded during heating stage and the theoretical best fitted curves. The curves were recorded at 25.5°C, 57.5°C and 93.5°C, respectively, *i.e.* at the lowest, the middle and the highest temperature of this range. As one can see, the theoretical curves are well fitted to the experimental ones in a broad range of the scattering vector s. In the case of the remaining 4 curves recorded in the temperatures 95.5–101.5°C, close to the complete melting of the copolymer, the quality of fit is somewhat worse as it can be seen in Fig. 4.

Generally, it can be concluded that the split Gauss function with an adjustable asymmetry factor n can be successfully used to describe the distribution function $P(\varphi)$ in a broad range of temperatures both during crystallization [8] and melting.

This conclusion has been additionally checked by a comparison of the results given by the Intensity Superposition Method with those ones obtained from the one-dimensional correlation function which was calculated for each curve using the method developed by Strobl & Schneider [1].

At first, based on the optimal parameters φ_m, σ and n found from the curve fitting method, the number average volume crystallinity φ_s was calculated for each temperature:

$$\varphi_s = \int\limits_{-\infty}^{\infty} \varphi P(\varphi)\mathrm{d}\varphi = \varphi_m + \frac{2\sigma(n-1)}{\sqrt{2\pi}} \qquad (8)$$

and compared with the average volume crystallinity obtained from the one dimensional correlation function – Fig. 5.

Next, using φ_s and the optimal average thickness of crystalline lamellae C_0 found from the curve fitting method, the average long period ($L_0 = C_0/\varphi_s$) and the average thickness of amorphous layers ($A_0 = L_0 - C_0$) were calculated for each temperature.
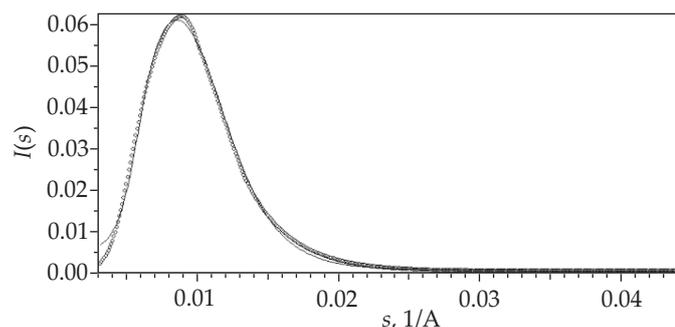
Fig. 1. Experimental one-dimensional scattering curve $I_1(s)$ curve – white circles – recorded at 25.5°C and best fitted theoretical curve – solid line – calculated by means Intensity Superposition Method
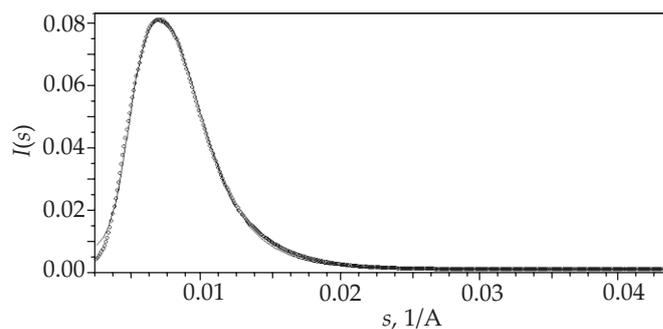

Fig. 2. Experimental one-dimensional scattering curve $I_1(s)$ curve – white circles – recorded at 57.5°C and best fitted theoretical curve – solid line – calculated by means Intensity Superposition Method
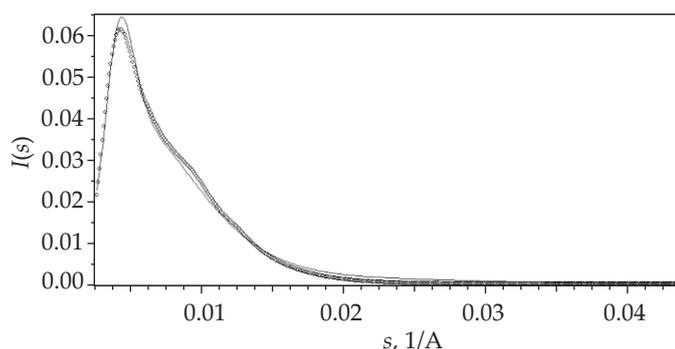

Fig. 3. Experimental one-dimensional scattering curve $I_1(s)$ curve – white circles – recorded at 93.5°C and best fitted theoretical curve – solid line – calculated by means Intensity Superposition Method
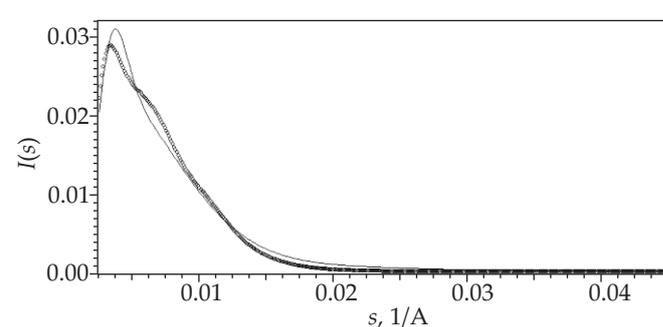

Fig. 4. Experimental one-dimensional scattering curve $I_1(s)$ curve – white circles – recorded at 101.5°C and best fitted theoretical curve – solid line – calculated by means Intensity Superposition Method
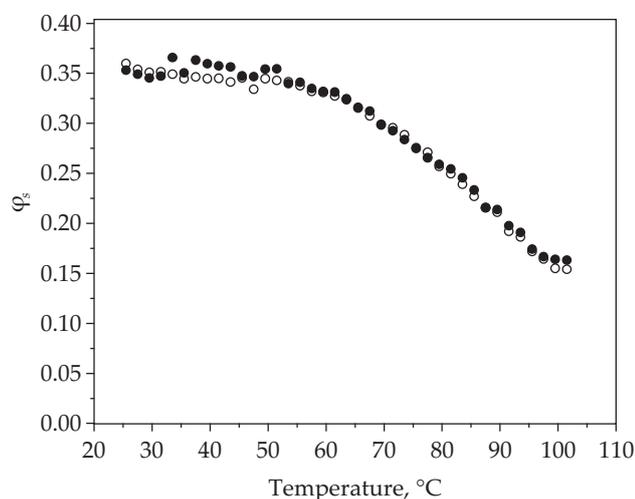

Fig. 5. Average volume crystallinity of stacks φ_s determined by means of the Intensity Superposition Method – white circles – and obtained from the one dimensional correlation function calculated for the SAXS curves – black circles
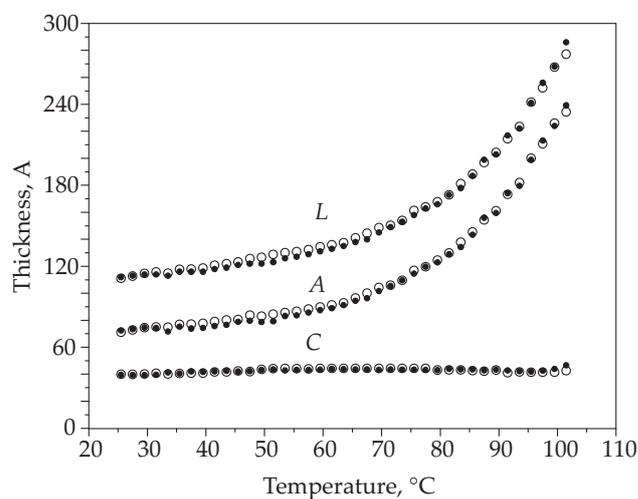

Fig. 6. Average values of long period (L), thickness of amorphous layer (A) and thickness of crystalline lamellae (C) determined by means of the Intensity Superposition Method – white circles – and obtained from the one dimensional correlation function calculated for the SAXS curves – black circles

Figure 6 presents these parameters of stacks for all SAXS curves recorded during heating compared with the related parameters calculated from the one dimensional correlation function. Both Fig. 5 and Fig. 6 show that the parameters of stacks determined with the two methods are nearly the same in the whole range of temperatures. It should be emphasized that good agreement is observed even for the data related to the highest temperatures 95.5–101.5°C, close to the complete melting of the copolymer, at which the quality of fit was somewhat worse (Fig. 4).
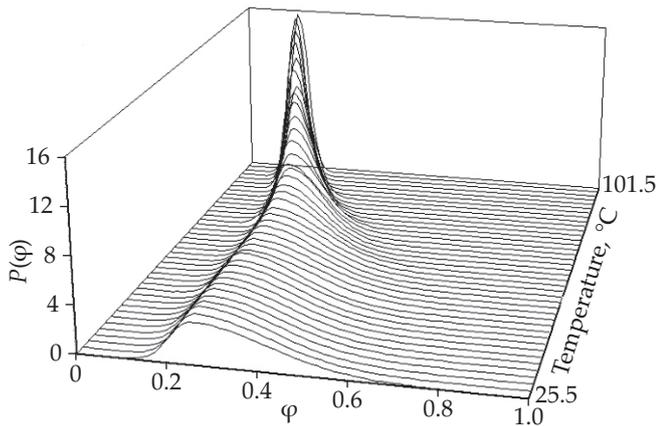
Fig. 7. Changes of the shape of the $P(\varphi)$ crystallinity distribution function during heating of the copolymer from 25.5 to 101.5°C

Performed comparison fully confirms the conclusion on the appropriate form of $P(\varphi)$ function assumed in our model calculations.

So, observing the shape of this function at different temperatures we can trace changes in the crystallinity distribution of stacks during heating of the copolymer. A general view of the $P(\varphi)$ function in the whole range of temperatures is shown in Fig. 7. As it can be seen, at the beginning of the heating stage the $P(\varphi)$ distribution is very broad and visibly asymmetric. It means that the copolymer is considerably inhomogeneous in terms of the lamellar stacks' crystallinity and structure. When the temperature increases, the distribution becomes more and more narrow.

At first sight the changes in the shape of $P(\varphi)$ distribution heating of the copolymer are exactly reverse with respect to those observed during cooling stage [8].

To characterize the changes quantitatively two parameters can be used: standard deviation σ_T of $P(\varphi)$ distribution calculated from Equation (9) and Pearson's skewness coefficient S [14], defined by Equation (10):

$$\sigma_T = \sqrt{\int_0^1 (\varphi-\varphi_s)^2 P(\varphi)\mathrm{d}\varphi} \approx \sqrt{\int_{-\infty}^{\infty} (\varphi-\varphi_s)^2 P(\varphi)\mathrm{d}\varphi} = \tag{9}$$

$$= \sigma\sqrt{(n-1)^2\left(1-\frac{2}{\pi}\right)+n}$$

$$S = \frac{\varphi_S - \varphi_m}{\sigma_T} \tag{10}$$

Figure 8 shows a comparison of the standard deviation σ_T during cooling and heating runs.

The standard deviation systematically increases during cooling from about $\sigma \approx 0.027$ at 89.5°C to $\sigma_T \approx 0.109$ at 25.5°C and decreases in the same rage while heating. At the lowest and the highest temperatures of this range σ_T is nearly the same both in cooling and heating run. So it means that the statistical dispersion of the crystallinity of stacks at these temperatures is similar during heating and cooling.
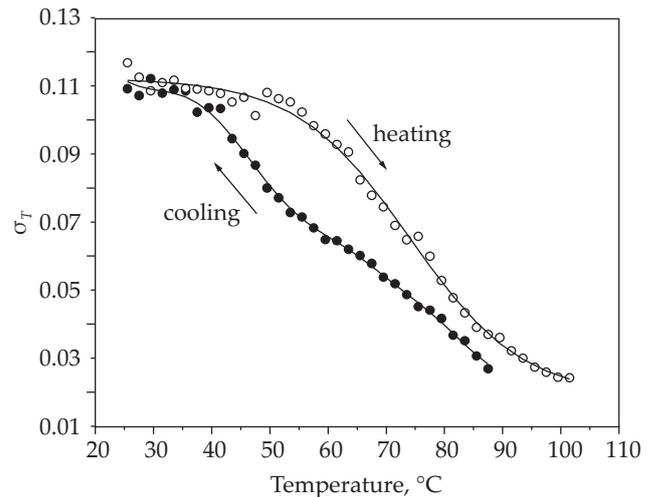

Fig. 8. Standard deviation σ_T of the $P(\varphi)$ crystallinity distribution function versus temperature during cooling – black circles – and heating – white circles – of the copolymer

The Pearson's skewness coefficient S shown in Fig. 9 behaves in different way. In the first period of cooling the coefficient is high ($S \approx 1.13$) and nearly constant, but below 60°C it starts to decrease reaching the value of about 0.98 at 25.5°C. During heating, this trend does not reverse like in the case of the standard deviation σ_T. On contrary, the Pearson's skewness coefficient S continues to decrease down to $S \approx 0.173$ at 101.5°C. Observed changes indicate that during heating the $P(\varphi)$ function becomes not only more and more narrow but also more and more symmetric. This fact is clearly visible in Fig. 10 which shows the $P(\varphi)$ distribution function at three temperatures: 25.5, 57.5 and 101.5°C.

Figure 11 presents a comparison of the $P(\varphi)$ distribution functions at the same temperature of 87.5°C during cooling and heating runs. As it could be expected, the value of φ for which the $P(\varphi)$ reaches its maximum and the number average crystallinity of stacks φ_s are lower during cooling than during heating. This fact is caused
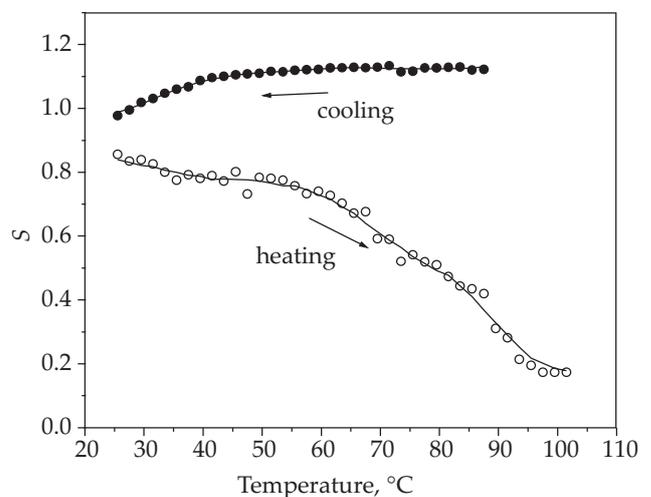

Fig. 9. Pearsons' skewness coefficient S of the $P(\varphi)$ crystallinity distribution function versus temperature during cooling – black circles – and heating– (white circles – of the copolymer
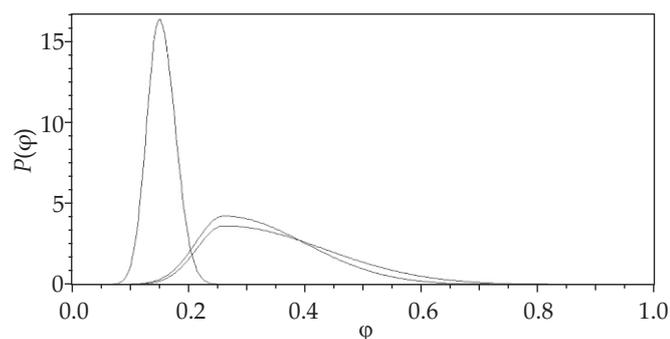
Fig. 10. The $P(\varphi)$ crystallinity distribution function at the temperatures $T = 25.5°C$ (1) 57.5°C (2) and 101.5°C (3) during heating of the copolymer

Fig. 11. A comparison of the $P(\varphi)$ crystallinity distribution function at the same temperature $T = 87.5°C$ during crystallization (1) and melting (2) of the copolymer; the number average volume crystallinity values φ_s related to the two functions are denoted by dashed lines

by the nucleation processes due to which the crystallization of a polymer always occurs at lower temperature than melting. But besides we see, that when the crystallization starts, the $P(\varphi)$ distribution function is very narrow and considerably asymmetric. Before melting the $P(\varphi)$ is narrow as well but almost completely symmetric.

The comparison proves evidently that the structure of lamellar stacks population at the beginning of crystallization and before melting differ considerably from one another in spite of the same temperature of the copolymer.

SUMMARY

The analysis of the SAXS curves of ethylene-1-octene copolymer accomplished in this work confirmed that both during melting and crystallization from the melt, the crystallinity distribution of lamellar stacks $P(\varphi)$ could be very well approximated by a positively skewed split Gauss function.

The observations of the changes in the shape of $P(\varphi)$ distribution were useful in a comparison of the structure of the lamellar stacks population during melting and crystallization of the copolymer.

At the highest temperatures, when the crystallization starts, the $P(\varphi)$ function is very narrow and highly asymmetric (Fig. 11) showing that generally the volume crystallinity of most stacks is very low but in some stacks it reaches much bigger values. When the temperature decreases new stacks of higher crystallinity appear and simultaneously the crystallinity of stacks formed at the first stages of crystallization increases thanks to the insertion of new lamellae between the older ones. As a consequence the $P(\varphi)$ distribution becomes broader and less asymmetric (Figs. 8 and 9) The increase in the standard deviation of $P(\varphi)$ distribution indicates that the copolymer becomes more inhomogeneous in terms of the stacks' structure. Such a trend is continued till the complete solidification at 25.5°C.

At the beginning of the heating stage the $P(\varphi)$ distribution is broad and still visibly asymmetric (Fig. 10). During heating the standard deviation of $P(\varphi)$ start to change in
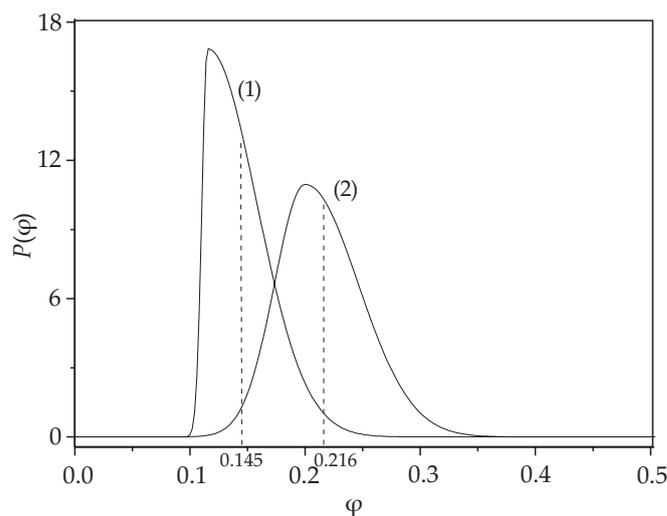
reversed direction (Fig. 8), but the skewness coefficient does not change its former trend – its value continues to decrease (Fig. 9). Finally, before complete melting the $P(\varphi)$ distribution is narrow again and only very slightly asymmetric (Figs. 10 and 11). What could be the reason of such a tendency? It is obvious that during heating, the thinnest and most defective lamellae melt first. The decrease in the skewness coefficient of positively skewed $P(\varphi)$ distribution indicates that the number of stacks of the highest crystallinity decreases. This means that the majority of thin and defective lamellae are located in stacks of the highest crystallinity. Most probably they were formed by the insertion mechanism. This is why the number of stacks of the highest crystallinity decreases rapidly with increasing temperature and as a result the $P(\varphi)$ distribution becomes narrow and more symmetric.

Obtained results indicate that the structure of the lamellar stacks population before melting is evidently different than at the beginning of crystallization.

Performed investigations have shown that the method of determination of the parameters of lamellar stacks in semicrystalline polymers employed in this work broadens considerably the information obtained from the analysis of SAXS curves. The Intensity Superposition Method allows to find not only the average values of the long period, the thicknesses of crystalline lamellae and amorphous layers but also the $P(\varphi)$ function which describes the distribution of crystallinity of lamellar stacks. Knowing the shape of this function and its parameters we can evaluate quantitatively the homogeneity of the polymer. Moreover, tracing the $P(\varphi)$ distribution we obtains additional information on the changes in the structure of the stacks population during thermal processes to which the polymer undergoes.

REFERENCES

[1] Strobl G.R., Schneider M.J.: *Journal of Polymer Science Part B: Polymer Physics* **1980**, *18*, 1343.
http://dx.doi.org/10.1002/pol.1980.180180614

[2] Vonk C.G., Kortleve G.: *Kolloid-Zeitschrift und Zeitschrift für Polymere* **1967**, *220*, 19.
http://dx.doi.org/0.1007/BF02086052

[3] Hermans J.J.: *Recueil des Travaux Chimiques des Pays-Bas* **1944**, *63*, 211.

[4] Hosemann R., Bagchi S.N.: „Direct Analysis of Diffraction by Matter", Amsterdam: North Holland 1962.

[5] Ruland W.: *Journal of Applied Crystallography* **1971**, *4*, 70.
http://dx.doi.org/10.1107/S002188987100709X

[6] Rabiej S., Rabiej M.: *Journal of Applied Crystallography* **2007**, *40* (*1–4*), 605.
http://dx.doi.org/10.1107/S0021889806056007

[7] Rabiej S., Rabiej M.: *Polimery* **2014**, *59,* 549.
http://dx.doi.org/10.14314/polimery. 2014.549

[8] Rabiej S., Rabiej M., Adamczyk-Tomiak K.: *European Polymer Journal* **2015**, *69*, 247.
http://dx.doi.org/10.1016/j.eurpolymj.2015.06.011

[9] Blundell D.J.: *Polymer* **1978**, *19*, 1258.
http://dx.doi.org/10.1016/0032-3861(78)90302-6

[10] Koberstein J.T., Morra B., Stein R.S.: *Journal of Applied Crystallography* **1980**, *13*, 34.
http://dx.doi.org/10.1107/S00218898 80011478

[11] Crist B.: *Journal of Macromolecular Science: Physics* **2000**, *B39*, 493.
http://dx.doi.org/10.1081/MB-100100401

[12] Rabiej M.: *Journal of Applied Crystallography* **2017**, *50* (*1*), 221.
http://dx.doi.org/10.1107/S160057671601983X

[13] Rabiej S., Rabiej M.: *Polimery* **2011**, *56*, 662
http://dx.doi.org/10.14314/polimery.2011.662

Received 3 III 2020

Rapid Communications

Przypominamy Autorom, że publikujemy artykuły typu **Rapid Communications – prace oryginalne wyłącznie w języku angielskim** (o objętości 4–5 stron maszynopisu z podwójną interlinią, zawierające 2–3 rysunki lub 1–2 tabele), którym umożliwiamy szybką ścieżkę druku (do 3 miesięcy od chwili ich otrzymania przez Redakcję). Artykuł należy przygotować wg wymagań redakcyjnych zamieszczonych we wskazówkach dla P.T. Autorów.

*   *   *

We remind Authors that we publish articles of the **Rapid Communications** type – **the original papers, in English only** (with a volume of 4-5 pages of double-spaced typescript, containing 2–3 figures or 1–2 tables), which allow a fast print path (up to 3 months from when they are received by the Editorial Board). The article should be prepared according to the editorial requirements included in the Guide for Authors.